Future Journal of Pharmaceutical Sciences

RESEARCH Open Access

Synthesis, characterization, and biological studies of some biometal complexes

Vinay Kumar Srivastava

Abstract

Background: Metal complexes $Cu[C_{13}H_8O_4N]_2$ **2,** $Ni[C_{l3}H_8O_4N]_2$ **3,** and $Co[C_{13}H_8O_4N]_2$ **4** of bioinorganic relevance have been synthesized with the Schiff base ligand 2-furylglyoxal–anthranilic acid (FGAA) $[C_{13}H_9O_4N]$ **1**.
All the complexes are well characterized by various spectral and physical methods. The antimicrobial activity of the complexes has been studied against some of the pathogenic bacteria and fungi.

Results: Results indicate that complexes have higher antimicrobial activity than the free ligand. This would suggest that chelation reduces considerably the polarity of the metal ions in the complexes which in turn increases the hydrophobic character of the chelate and thus enables permeation, through the lipid layer of microorganisms. All the complexes were assessed for their anticancer studies against a panel of selected cancer cells HOP62 and BT474 respectively. Results showed that the complexes are promising chemotherapeutic alternatives in the search of anticancer agents. The fluorescence quenching phenomenon is observed in the Schiff base metal complexes.

Conclusion: The octahedral transition metal complexes **2, 3,** and **4** have been obtained by treatment of ligand 2-furylglyoxal-anthranilic acid (FGAA) **1** with metal acetate. Complexes under investigations have shown antimicrobial, potential anticancer, and the DNA binding studies.

Keywords: Metal complexes, Characterization, Antimicrobial, Anticancer activity, DNA binding

Background

The chemistry of transition metal complexes has received considerable attention largely due to their catalytic and bioinorganic relevance. Such complexes are also important due to their potential biological activities such as antibacterial, antifungal, antimalarial, and antitumor [1–4]. Medicinal inorganic chemistry is comparatively a new discipline which developed after the serendipitous discovery of the antitumor activity of cisplatin [5–7]. The clinical success of this platinum complex has stimulated considerable interest in the search for new metal complexes as modern therapeutics, diagnostic, and radiopharmaceutical agents. Copper, nickel, and cobalt complexes are used in the treatment of many diseases including cancer and as potential hypoxia-activated prodrugs [8–14]. Coordination compounds which form coordinate bonds via the sulfur, oxygen, and nitrogen donor atoms are well known and have a long history. The interest in preparation of new metal complexes gained the tendency of studying the interactions of metal complexes with DNA for their applications in biotechnology and medicine.

Deoxyribonucleic acid (DNA) is the primary target molecule for most anticancer and antiviral therapies according to cell biologists. Investigation on the interaction of DNA with small molecules is important in the design of new type of pharmaceutical molecule. Schiff base constitutes an important class of nitrogen donor ligands and occupy a prominent position among the recent achievement in the field of coordination chemistry. The azomethine which is the functional group of Schiff base is aided in forming a stable complex. The chemistry of Schiff base metal complexes is exploited in industries,

Correspondence: vkschemistrydscollege@gmail.com
Chemical Research Laboratory, Faculty of Science, Department of Chemistry, DS College Aligarh, Dr. BR Ambedkar University, Agra, India

Table 1 Physical and analytical data of complexes 2, 3, and 4

S. no.	Compound	Color	% analysis		Found/(Calcd)		DT (°C)	Molar conductance ohm^{-1} cm^2 mol^{-1}
			C	H	N	M		
1	**2**	Dark brown	56.90 (56.98)	2.82 (2.92)	4.81 (4.87)	11.52 (11.62)	245.247	7.26
2	**3**	Brown	57.62 (57.49)	2.69 (2.95)	5.02 (5.16)	10.90 (10.82)	302	7.50
3	**4**	Brown	57.39 (57.46)	2.80 (2.94)	5.04 (5.16)	10.94 (10.85)	> 310	11.85

technologies, and in medicinal fields. The present investigations deal with the synthesis, characterization, antimicrobial, anticancer, and DNA cleavage studies of Cu(II), Ni(II), and Co(II) metal complexes containing Schiff base ligand 2-furylglyoxal-anthranilic acid (FGAA).

Methods

All reagents used were of analytical grade and used as purchased commercially; however, the solvents were purified by the standard procedure [15]. The ligand 2-furylglyoxal-anthranilic acid (FGAA) was prepared by the reported procedure [16–20]. C, H, and N were analyzed on Carlo-Erba microanalyzer. Metal contents were estimated by standard procedure [21]. FTIR was recorded on Thermo Nicolet Avater 370. Electronic spectra on Shimadzu UV-160A spectrophotometer. The conductance measurements were carried out on a metal CM-180 Eliodigital conductivity meter. Magnetic studies were done by a Guoy balance using Hg [Co $(SCN)_4$] as the calibrant.

^{1}H and ^{13}C NMR spectra in dimethyl sulfoxide (DMSO) were recorded on a Brucker WH 300 (200 MHz) and Varian Gemini (200 MHz) spectrometers using tetramethylsilane (TMS) as an internal reference.

The in vitro antimicrobial screening effects of the investigated compounds were tested against the bacterial species: *Escherichia coli*, (*E. coli*) and *Klbsiella pneumoniae* (*K. pneumoniae*), and fungal species: *Aspergillus niger* (*A. niger*) and *Candida albicans* (*C. albicans*) by using Kirby Bauer Disk diffusion method [22–24]. Chloramphenicol and nystatin were used as the standard antibacterial and antifungal agents. The tested compounds were dissolved in DMF solution (which has no inhibition activity) and solution soaked in filter paper disk of 5 mm diameter and 1 mm thickness. The disks

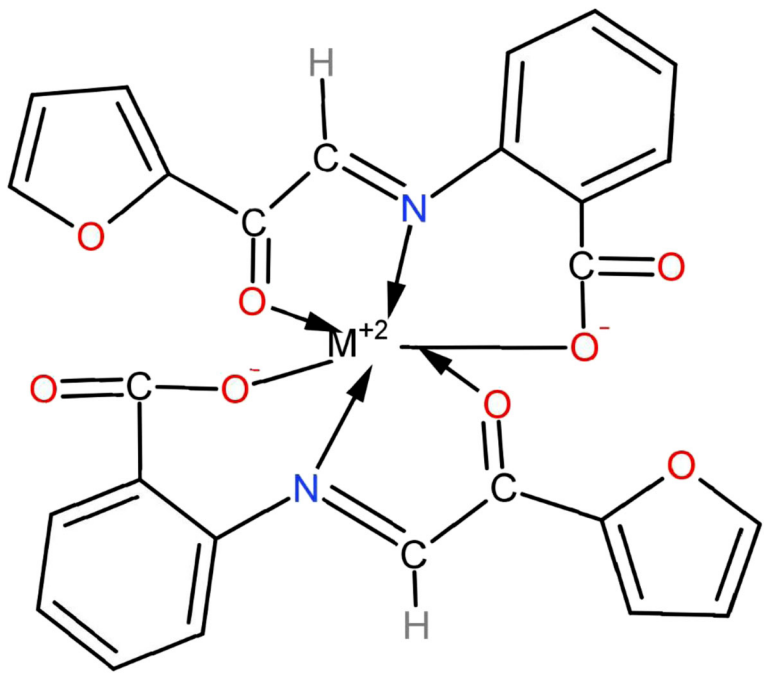

Fig. 1 The proposed structure of metal complex M = Cu(II) or Ni(II) or Co(II)

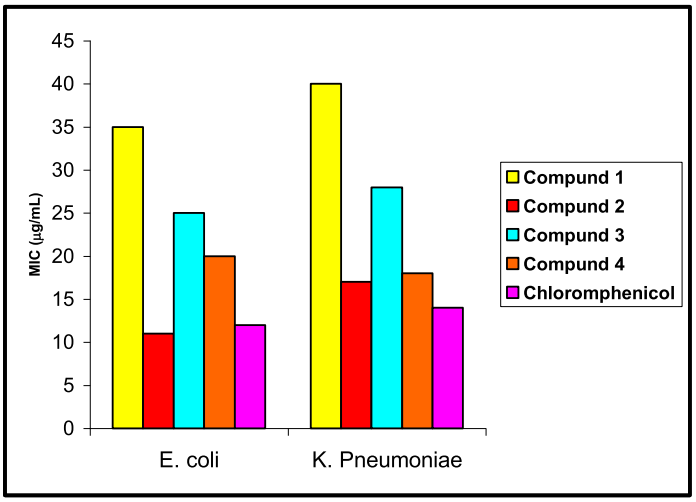

a Antibacterial Studies of Ligand and Its Metal Complex against E. coli and K. Pneumoniae

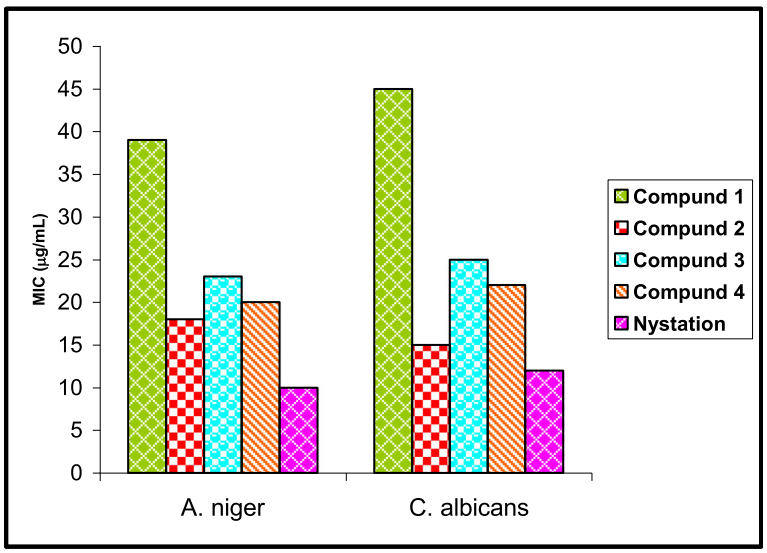

b Antifungal Studies of Ligand and Its Metal Complex against A. niger and C. albicans

Fig. 2 **a** Antibacterial studies of ligand and its metal complex against *E. coli* and *K. pneumoniae*. **b** Antifungal studies of ligand and its metal complex against *A. niger* and *C. albicans*

were incubated 24 h for bacterial and 72 h for fungal species at 37 °C. The minimum inhibitory concentration (MIC) value of the compounds was determined by the serial dilution method [25–27].

The in vitro cancer studies of all the compounds were assessed for their anti-proliferation test against a panel of selected human cancer cell lines such as HOP62 (lung) and BT 474 (breast) by using SRB (sulforhodamine B) assay [28–37] concentration of drug used 10, 20, 40, and 80 µg/mL ADR (adrimycin) was used as a positive control which controls cells with definite structure and clear cell wall without degeneration. Each drug was assayed inducing 50% growth inhibition (GI_{50}), total growth inhibition (TGI), and 50% cytotoxicity (LC_{50}) after a 48 h incubation period were calculated by linear interpolation from the observed data points. Fluorescence measurements were recorded on an F-7000 FL spectrophotometer at room temperature.

Table 2 Antimicrobial activity (MIC μg/mL) data

S. no.	Compound	Compound no.	Antibacterial activity		Antifungal activity	
			E. coli	*K. pneumoniae*	*A. niger*	*C. albicans*
1	Ligand	**1**	35	40	39	45
2	Cu $[C_{13}H_8O_4N]_2$	**2**	11	17	18	15
3.	Ni $[C_{13}H_8O_4N]_2$	**3**	25	28	23	25
4.	Co $[C_{13}H_8O_4N]_2$	**4**	20	18	20	22
5.	Chloramphenicol	**5**	12	14	—	—
6.	Nystatin	**6**	—	—	10	12

Synthesis of metal complexes (2-4)

Metal complexes of $Cu[C_{13}H_8O_4N)_2$ **2,** Ni $[C_{13}H_8O_4N]_2$ **3**, and Co $[C_{13}H_8O_4N]_2$ **4,** were synthesized by the addition of ethanolic solution of ligand 2-furylglyoxal–anthranilic acid **1** (2 mmol) copper acetate/nickel acetate/cobalt acetate (1 mmol). The mixture was magnetically stirred and refluxed for 2 h. The complexes obtained were filtered, washed with ethanol, and dried.

Results

All the metal complexes were colored, non-hygroscopic in nature, and stable at room temp. They were insoluble in common organic solvents but soluble in DMF and DMSO. The results of the elemental analysis are in good agreement with the calculated values. The molar conductance value indicates their non-electrolytic nature. Physical and analytical data of complexes are summarized in Table 1.

On the basis of analytical and spectral data, octahedral geometry has been assigned to the complexes. The results of antimicrobial activity and anticancer studies indicate metal complexes are much more active as compared to ligand fragments. Fluorescence quenching phenomena are observed in its metal complexes by fluorescence studies.

Discussion

IR spectral studies

Infrared spectra of free ligand, a sharp band [38–40] appeared at 1615-1590 cm^{-1} ascribed to the stretching vibrations of azomethine group and was shifted to lower frequency region after complexation suggesting thereby the participation of imine nitrogen. A strong band appeared at 1735-1690 cm^{-1} in the IR spectra of ligand (FGAA) which is due to the presence of stretching vibration of carbonyl group coordination through this carbonyl oxygen to the central metal ion is confirmed by a negative shift in this frequency in the spectra of corresponding metal complexes. IR spectra of ligand displays a bond of medium intensity in the region of 3550-3490 cm^{-1} due to the –OH stretching vibration of free $–CO_2H$ group. Coordination of ligand as a consequence of deprotonation of $– CO_2H$ group is evident by the disappearance of the above band in the IR spectra of respective complexes [41, 42]. Furthermore, the asymmetrical and symmetrical vibrations of COO^- group appeared at 1560-1535 cm^{-1} and 1340-1325 cm^{-1} Δν (as–s) value 220-210 cm^{-1} further indicate the coordination through unidentate carboxylate group. Some new bands appeared in the IR spectra of metal complexes at 550-530 cm^{-1}, 450-430 cm^{-1}, and 335-325 cm^{-1} are probably due to the formation of M–O, M–N, and M–S bonds respectively which further give additional evidences in favor of the coordination of metals

Table 3 % Control growth the drug concentrations (μg/mL) HOP62 cell line

Compound no.	Experiment 1				Experiment 2				Experiment 3				Average values			
	10	20	40	80	10	20	40	80	10	20	40	80	10	20	40	80
1	78.3	71.7	66.1	58.6	78.6	73.6	64.8	59.3	74.9	76.0	65.1	55.6	77.3	73.8	65.3	57.8
2	20.0	18.1	17.2	17.1	20.7	20.8	19.3	17.7	17.9	16.3	16.3	15.4	19.6	18.4	17.6	16.8
3	17.1	16.5	15.2	12.8	18.1	17.5	16.8	13.5	15.4	15.1	14.4	8.4	16.9	16.4	15.5	11.6
4	33.2	31.7	30.3	26.3	29.7	28.3	26.7	20.6	26.2	24.6	21.8	16.6	29.7	28.2	26.3	21.2
ADR	1.4	−5.1	−34.4	−34.8	−1.6	−5.9	−12.4	−35.8	−9.8	−14.4	−28.4	−41.1	−2.3	−8.5	−25.1	−37.2

Table 4 Parameters calculated from graph (Fig. 3) HOP62 cell line

Compound no.	Drug concentrations (μg/mL) calculated from graph		
	LC50	TGI	GI50
1	> 80	> 80	> 80
2	> 80	> 80	< 10
3	> 80	77.3	< 10
4	> 80	> 80	17.0
ADR	75.5	35.3	< 10

through azomethine nitrogen, carbonyl oxygen, and carboxylate group.

Electronic spectral and magnetic studies

Divalent copper having a d^9 configuration give rise to a 2D free ion term which split into a regular octahedral environment into a lower doublet ^2E_g and an upper triplet $^2T_{2g}$ levels. In electronic spectra [43–46] of a true octahedral system, only one band due to $^2E_g \rightarrow {}^2T_{2g}$ transitions is expected but true octahedral structures are not common. Therefore, instead of a one broad band due to $^2E_g \rightarrow {}^2T_{2g}$ transition. These transitions from the ground state $^2B_{1g} \rightarrow {}^2A_{1g} \rightarrow {}^2B_{2g}$ and ^2E_g are expected as a consequence of John-Tellers configuration stability. The ^2E_g orbitals separate so that one goes up as much as the other goes down.

The T_{2g} orbitals separate in such a way that the doubly degenerate pair goes down only half as far as the single orbital goes up therefore in case of Cu (II); there is no net energy change for T_{2g} electrons since four are stabilized while two are destabilized due to which Cu(II) complex shows distortion in an octahedral geometry. The electronic spectra of Cu(II) complex displays three spectral bands in the region 10635, 14850, 16345 cm^{-1} which are in good agreement with the distorted geometry of complex under investigation. This geometry is further supported by the magnetic moment value 1.98 B.M. of the complex. In the Ni(II) complex, three bands in the range 10750, 1665, 25650 cm^{-1} corresponding to the transition $^3A_{2g} \rightarrow {}^3T_{2g} \rightarrow {}^3T_{1g}$ and $^3T_{1g}(P)$ are observed which clearly indicate the octahedral geometry. The theoretical value of ν_2/ν_1 for octahedral Ni(II) complex is found 1.55. The observed value lies 1.60 which is in conformity with the distorted octahedral geometry of the ligand around central Ni(II) ion lowering the ratio of ν_2/ν_1 may be attributed due to configuration interaction between $T_{1g}(P)$ and $T_{1g}(F)$ excited state. The octahedral geometry is further supported by their magnetic value 3.14 B.M. In octahedrally surrounded Co(II) ions, three bands in the region 8000, 15616, 18175 cm^{-1} are expected which may be assigned to $^4T_{1g}$ to $^4T_{2g}$ (F) (ν_1), $^4A_{2g}(F)$ (ν_2), and $^4T_{1g}(P)$ (ν_3) transitions respectively. The $^4A_{2g}$

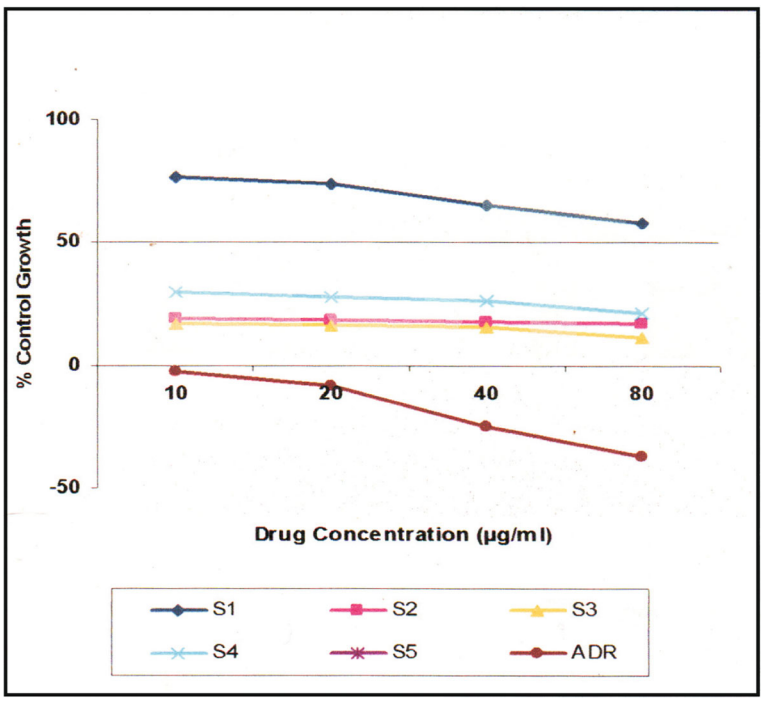

Fig. 3 Growth curve: human lung cancer cell line HOP 62 compounds **1-4**

Table 5 % Control growth the drug concentrations (μg/mL) BT474 cell line

Compound no.	Experiment 1				Experiment 2				Experiment 3				Average values			
	10	20	40	80	10	20	40	80	10	20	40	80	10	20	40	80
1	100.0	63.2	40.0	18.3	95.7	63.2	28.3	9.4	71.7	45.3	45.3	2.4	89-1	57.3	37.9	10.0
2	−15.2	−23.0	−24.0	−32.4	−17.1	−23.5	−26.9	−30.4	−25.5	−30.7	−30.9	−30.9	−19.3	−25.7	−27.3	−31.2
3	−27.5	−44.4	−50.4	−73.7	−28.9	−43.3	−44.2	−65.3	−36.0	−55.2	−65.8	−70.3	−30.8	−47.6	−53.4	−69.8
4	0.7	−9.9	−10.6	−13.8	3.0	−1.9	−3.5	−11.6	−6.3	−10.0	−11.1	−13.9	−0.9	−7.2	−8.4	−13.1
ADR	−25.8	−52.7	−66.4	−69.6	−16.2	−51.9	−66.8	−73.1	−26.2	−30.4	−70.0	−70.9	−22.7	−45.0	−67.7	−71.2

transition is very weak and often appears as shoulder. Cobalt complex possesses an octahedral geometry which is further confirmed by the energy ratio ν_2/ν_1 lies 1.95 and magnetic moment value 4.60 B.M.

NMR spectral studies

In the ^{1}H NMR spectra of free Schiff base ligand, the signals were appeared in the range of 7.15-7.20 ppm due to (HC=N) proton [47]. However, in the spectra of Schiff base metal complexes of Cu(II), Ni(II), and Co(II), the signals were observed in the downfield regions of 8.0–9.0 ppm supporting the coordination of iminonitrogen atom to Cu (II)/Ni (II)/Co (II) [48] while the free ligand NMR spectra has a characteristic NMR signal for carboxyl group proton in the 10.5-12.5 ppm range, the disappearance of this signal in the ^{1}H NMR spectra of metal complexes indicating the involvement of carboxylate ion oxygen in chelation through deprotonation. There is no appreciable change in the peak position corresponding to NH and aromatic protons. The ^{13}C–NMR signals for the metal, complexes are assigned by the comparison with the spectra of corresponding free Schiff base ligand. A downfield shift of CH = N group in the range of 150-160 ppm and for 175-182.5 ppm. In the complexes, NMR spectra indicate that the ligand coordinates through both the nitrogen atom of CH = N and the oxygen of COO^{-} ion [49–52] (Fig. 1).

In vitro antimicrobial studies

The antibacterial and antifungal activity of the ligand and complexes [53, 54] were assayed against some of the bacteria and fungi. DMF is used as negative control and chloramphenicol is used as a positive standard for antibacterial and nystatin for antifungal activities (Fig. 2a and b). The minimum inhibitory concentration (MIC) value of the compounds was determined by the serial dilution method and is given in Table 2.

The in vitro antimicrobial activity results revealed that complexes are more microbial toxic than the ligand. The activity order of the synthesized complexes and ligand are as follows **2 > 4 > 3 > 1**.

Such increased activity of the metal chelates can be explained on the basis of Tweedy's chelation theory on chelation, the polarity of the metal ion will be reduced to a greater extent due to the overlap of the ligand orbital and partial sharing of the positive charge of the metal ion with donor groups. Further, it increases the delocalization of π electrons over the whole chelate ring and enhances the penetration of the metal complexes into lipid membranes and blocking of the metal-binding sites in the enzymes of microogranism. These complexes also disturb the respiration process of the cell and thus block the synthesis of proteins which restricts further growth of the organism. The complex **2** shows higher antimicrobial activity than other complex **3** and **4** complex. The variation in the effectiveness of different compounds against different organisms depends either on the impermeability of the cells of the microbes or on differences in ribosome of microbial cells. Further, lipophilicity which controls the rate of entry of molecules into the cells is modified by coordination so compounds **2**, **3**, and **4** can become more active than compound **1** compared to the standard compounds chloramphenicol and nystatin (Fig. 2a and b); the present metal complexes are much less active against the representative strains of microorganism [55, 56].

Table 6 Parameters calculated from graph (Fig. 4) BT474 cell line

Compound no.	Drug concentrations (μg/mL) calculated from graph		
	LC50	TGI	GI50
1	> 80	> 80	38.9
2	78.1	30.3	< 10
3	51.0	17.3	< 10
4	> 80	46.4	< 10
ADR	49.1	17.5	< 10

In vitro anticancer studies

The data obtained by the SRB assay show that metal complexes **2** and **3** have inhibitory effects on the growth of HOP62 (Tables 3 and 4) (Fig. 3) and BT474 (Tables 5 and 6) (Fig. 4). Cancer cells in dose-dependent manner. Complex 4 exhibits cytotoxic effect on BT474 cancer cells but no antiproliferative effect against cell line

HOP62. The antiproliferative effect of tested complexes is likely due to the lipophilicity of the complexes that alleviate the transport of metal complexes into the cell and posteriorly into the organelles where metal may possibly contribute to toxicity by inhibitory cellular respiration and metabolism of biomolecules [57–59]. The pure metals are inactive however the activity of metal cations varies on their bioavailability hence delivery methods/solubility and ionization of metal sources are significant parameters to deal metals in biological system [60–62] possibly this is the reason that bonding of metal cations (Cu(II)/Ni(II)/Co(II) to biologically compatible ligand (FGAA) enhances the bioavailability and ultimately the activity of metal cations. In contrast, coordination enhances the activity of the metal complexes against BT 474 and HOP 62 cell lines. The compound **1** (ligand) exhibited no cytotoxic effect on both the cell lines. The choice of the coordinated ligand (s) seems to be as important as the choice of metal(s) because besides being the integral part of biologically active complexes. These organic molecules (ligands) can exert a biological activity of their own. The photomicrograph of the cells treated with compounds **1, 2, 3,** and **4** revealed the morphological features of apoptosis consist of membrane blebbing, nuclear condensation, cytoplasmic shrinkage, DNA fragmentation, cell wall destruction, and formation of apoptotic bodies (Figs. 5 and 6). Morphological images were grabbed using a phase-contrast microscope at × 20 magnifications with a digital camera at 48 h after treatment with the samples. Compound **1** showed negligible cytotoxicity as the cell growth and morphology did not get affected whereas it can be seen clearly that the compounds **2**, **3**, and **4** affected the normal morphology which rendered the cells to lose their viability. The picture revealed that the cells treated with compounds **2**, **3**, and **4** exhibited apoptotic cellular death as the population of cells reduced drastically within the 48 h of treatment. The photomicrograph depicts the treatment of HOP 62 and BT 474 cells treated with complexes **2**, **3**, and **4** showed a significant inhibitory effect on the cellular growth. In all two cell lines, the increase in the number of cells with abnormal morphology was accompanied by an increase in the number of irregular refractive clumps. The majority of the cell appear to be rounded and shrunken due to apoptosis and white spots in the images showing the apoptotic cell. The percentage cell viability in presence of ligand and metal complexes for BT 474 and HOP 62 cell lines are shown in Figs. 3 and 4. The graphs of percentage control growth versus molar drug concentration showed the effective drug concentration on both cell lines and each point is the mean standard error obtained from three independent experiments. The results showed that complexes **2**, **3**, and **4** were the most potent and strongly inhibited the proliferations of both the two cell lines in a dose-dependent manner with TGI values 17.3, 30.3, and 46.4 μg/ml respectively. It was verified that the increased in concentration of complexes leads to higher cytotoxic activities. Nevertheless, results also proved that ADR showed superior cytotoxic activity against both cell lines.

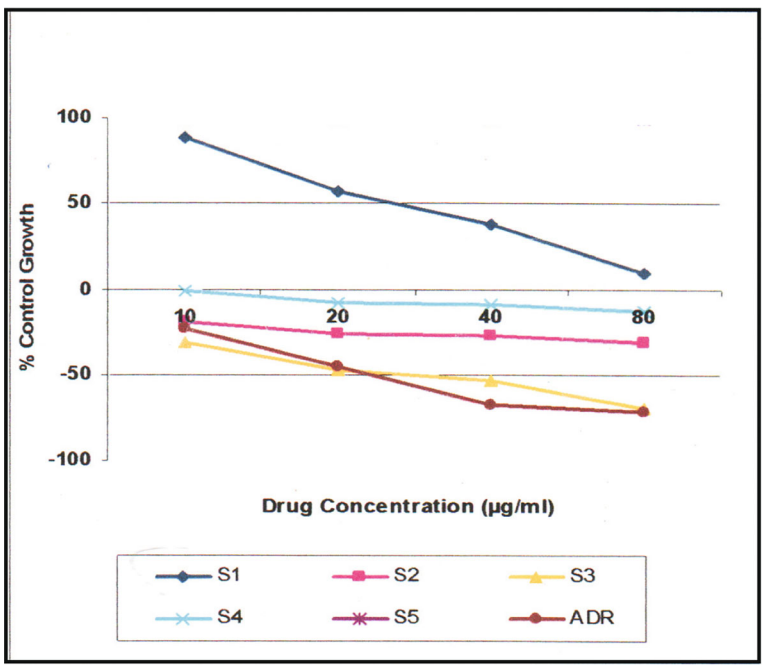

Fig. 4 Growth curve: human breast cancer cell line BT 474 compounds **1**-**4**

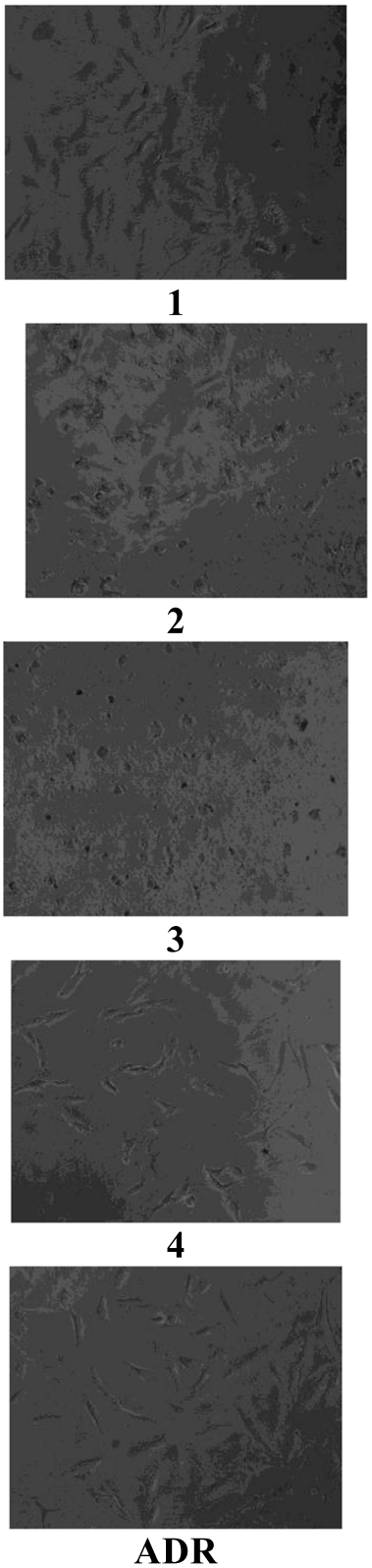

Fig. 5 HOP 62 Cell images compounds **1**-**4**

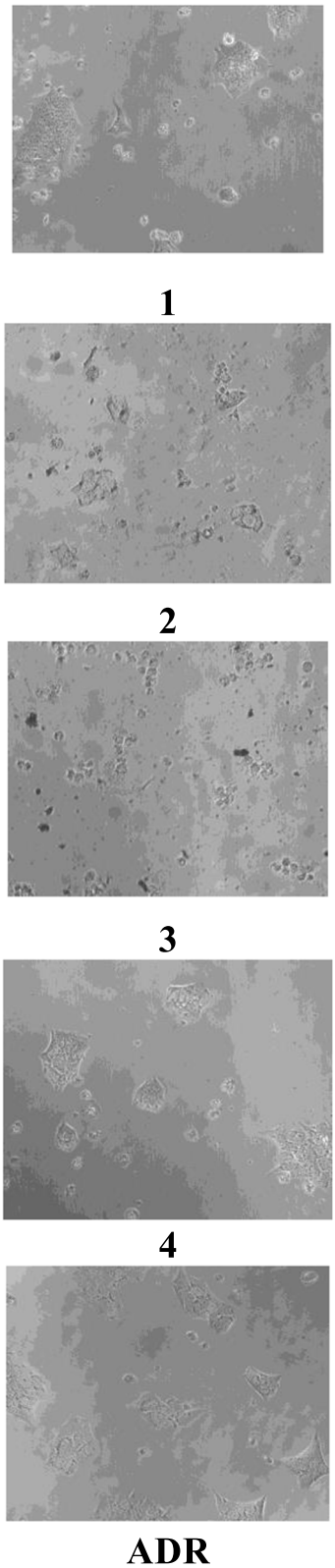

Fig. 6 BT474 Cell images compounds **1-4**

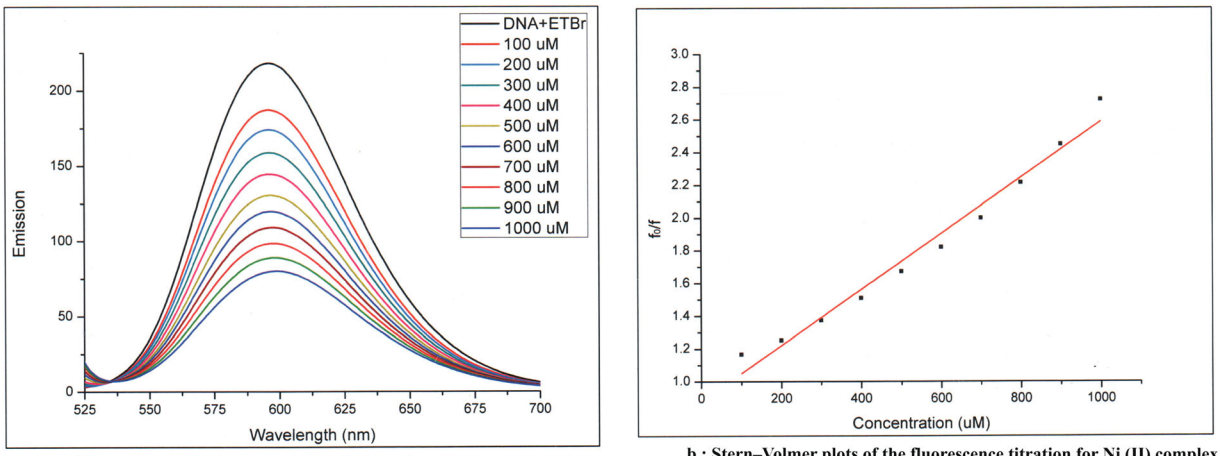

a : Fluorescence quenching curves of ethidium bromide bound to DNA in presence of Ni (II) complex.

b : Stern–Volmer plots of the fluorescence titration for Ni (II) complex. Representation of slope and Intercept values. Kb=slope/Intercept value i.e. 1.94 x $10^3 M^{-1}$ F_0=Highest emission of DNA+Ethr. F=Highest emission of DNA+Ethr after addition of complexes.

Fig. 7 a Fluorescence quenching curves of ethidium bromide bound to DNA in presence of Ni (II) complex. **b** Stern-Volmer plots of the fluorescence titration for Ni (II) complex. Representation of slope and Intercept values. Kb = slope/Intercept value i.e. 1.94 × $10^2 M^{-1}$ F0 = Highest emission of DNA+Etbr, F = Highest emission of DNA+Etbr after addition of complexes

Fluorescence studies

Emission intensity of the three complexes increases on increasing the conc. of CT DNA. The enhancement of emission intensity is an indication of binding for the complexes to the hydrophobic pockets of DNA and complexes can be protected efficiently by the hydrophobic environment inside the DNA helix [63, 64]. The high binding affinities of the metal complexes are probably attributed to the extension of the π system of the intercalated ligand due to the co-ordination of transition metal ions which also leads to a planar area greater than that of the free ligand and the coordinated ligand penetrating more deeply into and stacking more strongly with base pairs of DNA. The quenching plots illustrate that the quenching of ethidium bromide (EtBr) bound to DNA by the complexes are in good agreement with the linear Stern-Volmer equation which proves that the three complexes bind to DNA. The K_b (slope/intercept values in graph of F_0/F vs (conc.) values for complexes **2**, **3**, and **4** are 2.225 × 10^2 M^{-1}, 1.94 × 10^2 M^{-1}, and 1.55 × 10^2 M^{-1}). Based on the K_b values, the order of binding strength of metal complexes **2** > **3** > **4** (Figs. 7, 8, 9).

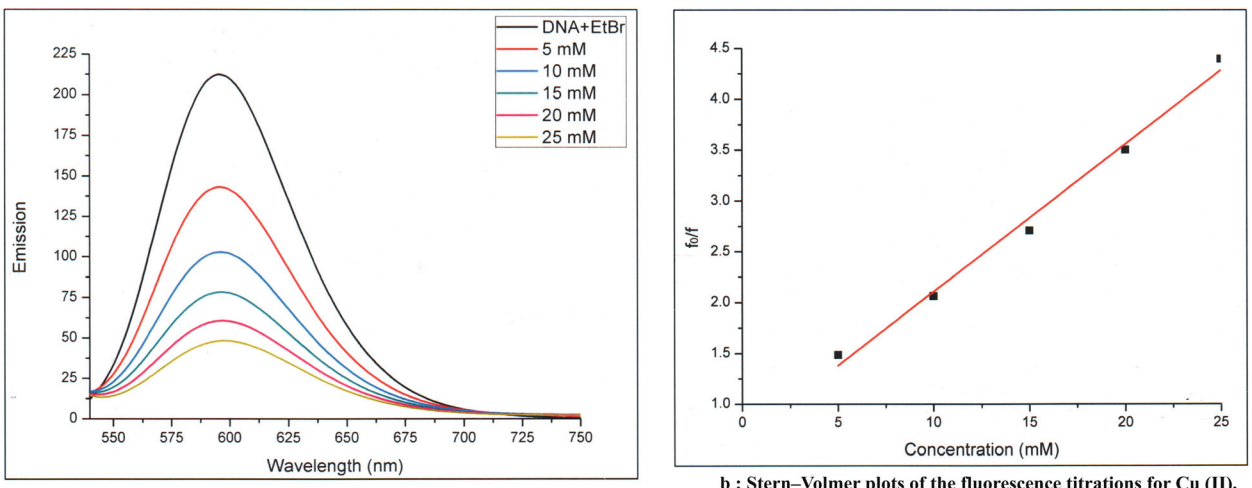

a : Fluorescence quenching curves of ethidium bromide bound to DNA in presence of Cu (II) Complex.

b : Stern–Volmer plots of the fluorescence titrations for Cu (II). Representation of slope and intercept values. Kb=slope / Intercept value i.e. 2.225x10^2 M^{-1}.

Fig. 8 a Fluorescence quenching curves of ethidium bromide bound to DNA in presence of Cu (II) Complex. **b** Stern-Volmer plots of the fluorescence titrations for Cu (II) Complex. Representation of slope and intercept values. Kb = slope/Intercept value i.e. 2.225 × 10^2 M^{-1}

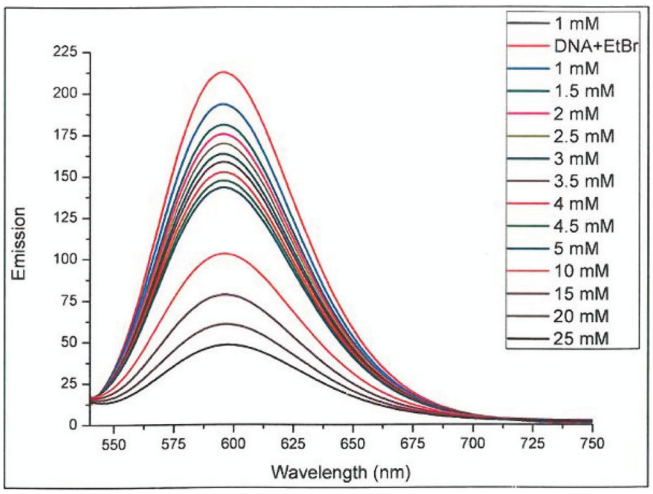

a : Fluorescence quenching curves of ethidium bromide bound to DNA in presence of Co (II) complex.

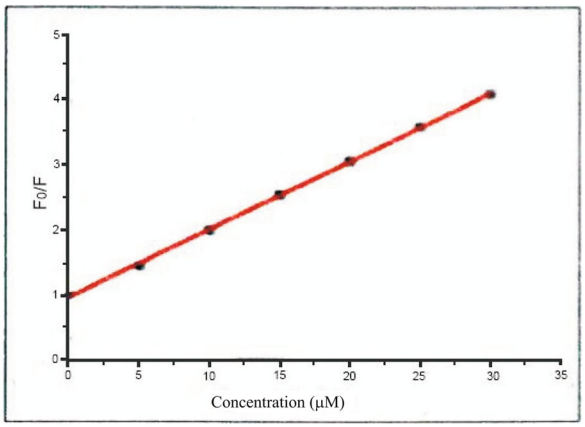

b : Stern–Volmer plots of the fluorescence titrations for Co (II). Representation of slope and intercept values. Kb=slope / Intercept value i.e. $1.55x10^2$ M^{-1}.

Fig. 9 a Fluorescence quenching curves of ethidium bromide bound to DNA in presence of Co (II) complex. **b** Stern-Volmer plots of the fluorescence titrations for Co (II) Complex. Representation of slope and intercept values. Kb = slope/Intercept value i.e. 1.55×10^2 M^{-1}

Conclusions

In the present study, novel metal complexes of Cu(II), Ni(II), and Co(II) were prepared and characterized by physico-chemical methods. Spectral studies demonstrate the ligand coordinating through azomethine nitrogen and carboxylate oxygen atoms and reveal octahedral geometry for Cu(II), Ni(II), and Co(II) complexes. The antibacterial and antifungal data given for the compound presented in this paper allowed us to state that the metal complexes generally have better activity than the ligands and less activity than standards. The metal complexes exerted growth inhibition on the human tumor cell lines showing promise as potential anticancer drugs deserving of further investigation. The Schiff base exhibits a strong fluorescence emission contrast to this partial fluorescence quenching phenomena is observed in its metal complexes.

Abbreviations

FGAA: 2-Furylglyoxal-anthranilic acid; TMS: Tera methyl silane; DMF: Dimethyl formamide; DMSO: Dimethyl sulfoxide; MIC: Minimum inhibitory concentration; SRB: Sulforhodamine B; ADR: Adrimycin; GI_{50}: 50% growth inhibition; TGI: Total growth inhibition; LC_{50}: Cytotoxic killing of 50% of cells

Acknowledgements

The author express his gratitude to the STIC, Cochin University, CDRI, Lucknow , S.P Centre for Science and Technology Vallabh Vidhya Nagar, and ACTREC Mumbai for providing facilities of spectral and biological studies.

Author's contributions

The author designed, performed experiments, analyzed data, and wrote the manuscript. The author read and approved the final manuscript.

Funding

Not applicable

Availability of data and materials

Available on request

Ethics approval and consent to participate

Not applicable

Consent for publication

Not applicable

Competing interests

The author has no conflict of interest.

Received: 26 August 2020 Accepted: 21 January 2021
Published online: 24 February 2021

References

1. Patole J, Dutta S, Padhye S, Sinn E (2001) Inorg Chim Acta 318:207
2. Maurer RI, Blower PJ, Dilworth JR, Reynolds CA, Zheng Y, Mullen GED (2002) J Med Chem 45:1420
3. Jouad EM, Thanh XD, Bouet G, Bonneaus, Khan MA (2002) Anti Cancer Res 22:1713
4. Cowly AR, Dilworth JR, Donnely PS, Labisbal E, Sousa A (2002) J Am Chem Soc 124:5270
5. Gray HB (2003) Proc Natl Acad Sci U S A 100:3563
6. Abrams MJ, Murrer BA (1993) Science 261:725
7. Rosenberg B, Vancamp L, Troska JE, Mansour VH (1969) Nature 222:385
8. Guo Z, Sadler P (2000) J Adv Inorg Chem 49:183–306
9. Cvek B, Milacic V, Taraba J, Dou QP (2008) J Med Chem 51:6256
10. Anderson RF, Denny WA, Ware DC, Wilson WR (1996) Br J Cancer 74:548
11. Teicher B, Abrams M, Rosbe K, Herman T (1990) Cancer Res 50:6971
12. Ware DC, Palmer HR, Brothers PJ, Rickard CEF, Wilson WR, Denny WA (1997) J Inorg Bichem 68:215
13. Wilson WR, Moselen JW, Cliffe S, Denny WA, Ware DC (1994) Int J Radiat Oncol Biol Phys 29:323
14. Ware DC, Palmer BD, Wilson WR, Denny WA (1993) J Med Chem 36:1839
15. Vogel AI, Furniss BS (1989) A text book of practical inorg chem, 5th edn. Longman, London
16. Kipnis F, Ornfelt J (1948) J Am Chem Soc 70:3948
17. Cai YH (2012) Asian J Chem 24(10):4468–4470
18. Elzahany E, Hegab K, Khalil S, Youssef N (2008) Aust J Basic Sci 2(2):210–220
19. Wang Q, Wang Y, Yang ZY (2008) J Chem Pharm Bull 56(7):1018–1021
20. Yong Feng Q, Lin D, Zhou J, Hu Y, Lin L, Li B, Qihua Z (2014) J Coord Chem 67(15):2615–2629
21. Vogel AI (1978) A text book of quantitative inorganic analysis Longman, London

22. Ferraari MB, Capacchis S, Reffo G, Tarasconi P, Albertini R, Pinelli S, Lunghi P (1999) Inorg Chim Acta 286:134–141
23. Pandaya SN, Sriram D (1999) Declercq. Eur J Pharm Sci 9:25–31
24. Bauer AW, Kirby WM, Sherris JC, Truck M (1966) Am J Clin Pathol 45:493–496
25. Avishai BD, Charles E, Davidson (2014) J Microbiol Methods 107:214–221
26. Hedges AJ (2002) Int J Food Microbiol 76:2002
27. Cullen JJ, MacIntyre HL (2016) J Appl Psychol 28(1):279–298
28. Fricker SP, Buckley RG (1996) Anticancer Res 16:3755–3760
29. Keepers YP, Pizao PE, Peters GJ, Arkeotte J, Winograd B, Pinedo HM (1991) Eur J Cancer 27:897–900
30. Papazisis KT, Geromichalos GD, Dimitriadis KA, Kortsaris AH (1997) J Immunol Methods 208:151–158
31. Griffon G, Merlin JL, Marchal C (1995) Anti-Cancer Drugs 6:115–123
32. Mosmann T (1983) J Immunol Methods 65(1-2):55–63
33. Jin M, Zhao W, ,Zhang Y, Kobayashi M, Duan H, Kong D (2011) Int J Mol Sci 12(11): 7352-7359.
34. Hui Y, Wei Z, Qing Y, Fuping H, Hedong B, Hong L (2017) Molecules 22(10): 3–10
35. Xiao YJ, Diao QC, Liang YH, Zeng K (2017) Braz J Med Biol Res 50:1–5
36. Wang FY, Tang XM, Wang X, Huang KB, Feng HW, Chen ZF, Liu YN, Liang H (2018) Eu J Med Chem 155:639–650
37. Latif MA, Tofaz T, ,Zahan KD (2019) Russ J Chem 89:1197-1201.
38. Iskander MF, Eisyed L, Ismail KZ (1979) Transit Met Chem 4:225
39. Thankamony M, Mohanan K (2007) Indian J Chem A 46:249
40. Thomas M, Nair MKM, Radhakrishan RK (1995) Synth React Inorg Met-Org Chem 25:471
41. Nakamoto K (1997) Infrared and Raman spectra of inorganic and coordination compounds. Wiley, New York
42. Xiu RB, Mintz FL, You XZ, Wang RX, Yue Q, Meng QJ, Luy J, Derveer DV (1996) Polyhedron 15:4585
43. Lever ABP (1968) Inorganic electronic spectroscopy. Elsevier, New York
44. Sharda LN, Ganorkar M (1988) Indian J Chem A 27:617
45. Warad DV, Satish CD, Kulkarini VH, Bajgur CS (2000) Indian J Chem A 39:415
46. Skoog DA, Holler F, James C, Stanley R (2007) Principles of instrumental analysis, 6th edn. Thomson Brooks Cole, Belmont, pp 169–173
47. Reddy PM, HO YP, Shankar K, Rohini R, Ravinder V (2009) J Coord Chem 44: 2621–2625
48. Prasad AV, Reddy PM, Shankar K, Rohini R (2009) Color Technol 125:284–287
49. Shankar K, Rohini R, Reddy PM, HO YP, Ravinder V (2009) J Coord Chem 62: 3040–3049
50. Bhave NS, Kharat RB (1980) J Inorg Nucl Chem 45:977
51. Gunther H (1995) NMR spectroscopy basic principles, concepts, and applications in chemistry, 2nd edn. Wiley
52. Freeman RA (1997) Handbook of nuclear magnetic resonance, Longman, Essex, 2nd ed.UK
53. Irobi ON, Moo-Young M, Anderson WA (1996) Int J Pharm 34:87
54. Pelczar MJ, Chan ECS, Krieg NR (1998) Microbiology Blackwell Science, New York
55. Win Y, Yousif E, Majeed A, Ha S (2011) Asian J Chem 23(11):5009–5012
56. Stokes EJ, Ridgway GL (1980) Clinical Bacteriology Edward Arnold Publisher Maryland USA
57. Singh AP, Kaushik NK, Verma AK, Hundal G, Gupta R (2009) Eur J Med Chem 44:2009
58. Verma AK, Bansal S, Singh J, Tiwari RK, Kasi Sonkar V, Tandon V, Chandra R (2006) Bio Org Med Chem 14:6733
59. Takara K, Obata Y, Yoshikawa E, Kitada N, Sakaeda T, Ohnishi N, Xokoyama T (2006) Cancer Chemother Pharmacol 58:785
60. Jevtovic V, Pelosi G, Ianelli S, Kuvacevic R, Kaisarevic S (2010) Acta Chim Slov 57:363–369
61. Loa J, Chow P, Zhang K (2009) Cancer Chemother Pharmacol 63:1007
62. Jiang S, Yan G, Way J (2000) J Chem Soc Dalton Trans:1431
63. Lakowicz JR (1999) Principles of fluorescence spectroscopy, 2nd edn. Kluwer Academic Press Planum Publishers, New York
64. Chem GJ, Huang XZ, Zheng ZZ, XU JG, Wang ZB (1990) Methods of fluorescence analysis, 2nd edn. Science Press, Beijing

Publisher's Note